The Journal of Biological Chemistry
AFFINITY SITES
ASBMB
American Society for Biochemistry and Molecular Biology

Protein Structure and Folding:

Crystal Structures of Four Types of Human Papillomavirus L1 Capsid Proteins: UNDERSTANDING THE SPECIFICITY OF NEUTRALIZING MONOCLONAL ANTIBODIES

Brooke Bishop, Jhimli Dasgupta, Michael Klein, Robert L. Garcea, Neil D. Christensen, Rui Zhao and Xiaojiang S. Chen

J. Biol. Chem. 2007, 282:31803-31811.
doi: 10.1074/jbc.M706380200 originally published online September 4, 2007

Access the most updated version of this article at doi: 10.1074/jbc.M706380200

Find articles, minireviews, Reflections and Classics on similar topics on the JBC Affinity Sites.

Alerts:
- When this article is cited
- When a correction for this article is posted

Click here to choose from all of JBC's e-mail alerts

Supplemental material:
http://www.jbc.org/content/suppl/2007/09/06/M706380200.DC1.html

This article cites 23 references, 12 of which can be accessed free at
http://www.jbc.org/content/282/43/31803.full.html#ref-list-1

Downloaded from http://www.jbc.org/ by guest on August 5, 2013

THE JOURNAL OF BIOLOGICAL CHEMISTRY VOL. 282, NO. 43, pp. 31803–31811, October 26, 2007
© 2007 by The American Society for Biochemistry and Molecular Biology, Inc. Printed in the U.S.A.

Crystal Structures of Four Types of Human Papillomavirus L1 Capsid Proteins

UNDERSTANDING THE SPECIFICITY OF NEUTRALIZING MONOCLONAL ANTIBODIES[*][S]

Received for publication, August 2, 2007, and in revised form, September 4, 2007 Published, JBC Papers in Press, September 4, 2007, DOI 10.1074/jbc.M706380200

Brooke Bishop[‡§1], **Jhimli Dasgupta**[‡1], **Michael Klein**[‡], **Robert L. Garcea**[¶], **Neil D. Christensen**[‖], **Rui Zhao**[§], **and Xiaojiang S. Chen**[‡2]

From the [‡]*Department of Molecular and Computational Biology, University of Southern California, Los Angeles, California 90089, the Departments of* [§]*Biochemistry and Molecular Genetics and* [¶]*Pediatric Hematology-Oncology, University of Colorado Health Sciences Center, Aurora, Colorado 80045, the* [‖]*Jake Gittlen Cancer Research Foundation, Department of Pathology, Microbiology, and Immunology, Penn State College of Medicine, Hershey, Pennsylvania 17033*

Human papillomaviruses (HPVs) are known etiologic agents of cervical cancer. Vaccines that contain virus-like particles (VLPs) made of L1 capsid protein from several high risk HPV types have proven to be effective against HPV infections. Raising high levels of neutralizing antibodies against each HPV type is believed to be the primary mechanism of protection, gained by vaccination. Antibodies elicited by a particular HPV type are highly specific to that particular HPV type and show little or no cross-reactivity between HPV types. With an intention to understand the interplay between the L1 structure of different HPV types and the type specificity of neutralizing antibodies, we have prepared the L1 pentamers of four different HPV types, HPV11, HPV16, HPV18, and HPV35. The pentamers only bind the type-specific neutralizing monoclonal antibodies (NmAbs) that are raised against the VLP of the corresponding HPV type, implying that the surface loop structures of the pentamers from each type are distinctive and functionally active as VLPs in terms of antibody binding. We have determined the crystal structures of all four L1 pentamers, and their comparisons revealed characteristic conformational differences of the surface loops that contain the known epitopes for the NmAbs. On the basis of these distinct surface loop structures, we have provided a molecular explanation for the type specificity of NmAbs against HPV infection.

Human papillomaviruses (HPVs)[3] are a family of double-stranded DNA viruses that infect epithelial cells in a tissue-specific manner. Some low risk human papillomaviruses such as types 6 and 11 cause benign condylomas, whereas the other types such as HPV16, 18, 31, 33, 35, and 45 are associated with the development of the cervical cancer. Two of these HPV types, HPV16 and HPV18, account for 60–70% of all cervical cancer cases worldwide (1, 2). Papillomavirus capsids contain two virally encoded proteins L1 and L2, synthesized late in the infection cycle, which encapsidate the histone-associated, closed circular double-stranded DNA minichromosome (3). The viral capsid is primarily composed of 72 pentamers (capsomeres) of the L1 protein, in association with 12 or more copies of the L2 protein. The major late protein L1 pentamers have the intrinsic property of self-assembly into empty capsids, referred to as virus like particles (VLPs) (4–8). VLPs are structurally and immunologically similar to infectious viruses, as determined by electron microscopy and their ability to bind conformation-dependent monoclonal antibodies (mAbs) (4).

High levels of neutralizing antibodies can be generated after immunization with HPV VLP (9). These neutralizing antibodies to L1 are highly type-specific (10). Sequence analyses of various human papillomaviruses show a high degree of homology between the major capsid proteins (L1s) of different papillomaviruses (see Fig. 1). Despite the similarity, type-specific antibody responses have been well documented in studies of genital HPV infections as well as animal model immunization studies.

Both linear and conformational epitopes have been identified on the surface of HPV L1 VLPs (11), and it is now well established that conformational epitopes are responsible for the activity of neutralizing antibody (12–14). The structure of the HPV16 T = 1 particle (VLP) was solved by Chen *et al.* (15), and from this structure it was suggested that the loops extending toward the outer surface of the capsomere contained the type-specific epitope(s). However, most of the HPV neutralization epitopes are conformation-dependent, and their surface localizations on VLPs as well as their amino acid compositions have not been identified. The identification of such epitopes has been done primarily by measuring the reactivity of the mAbs to the VLPs either after the site-directed mutagenesis of L1 or after the insertion of foreign peptides within the different hypervariable loops of the L1 protein (16, 17). For example, such studies suggested that an epitope composed of the FG

* This work was supported in part by National Institutes of Health Grants AI048747 (to X. S. C.), CA37667 (to R. L. G.), and CA47622 (to N. D. C.). The costs of publication of this article were defrayed in part by the payment of page charges. This article must therefore be hereby marked "*advertisement*" in accordance with 18 U.S.C. Section 1734 solely to indicate this fact.

[S] The on-line version of this article (available at http://www.jbc.org) contains supplemental Fig. S1.

[1] These authors contributed equally to this work.

[2] To whom correspondence should be addressed: Dept. of Molecular and Computational Biology, University of Southern California, 1050 Childs Way, RRH201, Los Angeles, CA 90089. Tel.: 213-740-5487; Fax: 213-740-4390; E-mail: Xiaojiang.Chen@USC.edu/.

[3] The abbreviations used are: HPV, human papillomavirus; mAb, monoclonal antibody; VLP, virus-like particle; NmAb, neutralizing mAb; GST, glutathione *S*-transferase; DTT, dithiothreitol; MES, 2-(*N*-morpholino)ethanesulfonic acid; MOPS, 3-(*N*-morpholino)propanesulfonic acid.

Downloaded from http://www.jbc.org/ by guest on August 5, 2013

TABLE 1
Data collection and refinement statistics

Data sets	HPV11	HPV16	HPV18	HPV35
Crystal cell parameters				
Space group	*C2*	$P2_12_12_1$	*P1*	$P2_1$
Cell dimensions				
a, *b*, *c* (Å)	115.6, 159.8, 158.2	105, 159.1, 413.7	81.1, 105, 235.7	150.4, 176.6, 197.1
β (°)	101.8		87.5, 85.6, 68.1	92.11
Data collection statistics				
Resolution range (Å)	51.6–3.2 (3.31–3.2)	50–3.7 (3.83–3.7)	49.9–3.4 (3.52–3.4)	50–3.3 (3.38–3.3)
Observations	145132	154538	350632	742968
Unique reflections	45624	60322	98881	119918
Average redundancy	3.18	2.56	3.55	6.19
Completeness (%)	98.3 (99.5)	80.4 (73.7)	99.8 (99.8)	94.0 (90.0)
R_{sym} (%, last bin)	19.2 (33.6)	11.6 (17.8)	19.6 (38.2)	18.9 (43.0)
I/σ (last bin)	5.5 (2.9)	2.7 (2.2)	4.4 (2.4)	2.6 (1.7)
Refinement statistics				
R_{cryst} (%)	25.8	24.7	25.24	29.5
R_{free} (%)	28.2	29.6	27.73	32.1
Root mean square deviation				
Bond length (Å)	0.010	0.012	0.010	0.009
Bond angle (°)	1.32	1.59	1.48	1.30

and HI loops is immunodominant for HPV16 (18), whereas mAb binding studies for HPV6 and HPV11 have indicated that the BC, DE, and HI loops are important for these two types (19, 20).

mAb binding studies with VLPs suggest that the conformation of the surface loops play important roles in determining the type specificity of neutralizing mAbs (NmAbs) for different HPV types. To understand the interplay between type specificity of NmAbs and the conformation of the L1 surface loops at the molecular level, we have determined the L1 pentameric structures of four different HPV types HPV11, HPV16, HPV18, and HPV35. The preservation of the distinctive surface features of these pentamers unique to each type are shown by the efficient binding of the type-specific NmAbs raised against the VLPs of the corresponding HPV type. We also show that although HPV16 L1 crystal structure from the free pentamer has the same surface loop disposition as that in the previously determined T = 1 particle structure, the L1 of HPV16 and each of the other types have distinct features on their pentameric surface, unique to each HPV type, that rationalize the type specificity of the NmAbs at the atomic level.

EXPERIMENTAL PROCEDURES

Cloning and Deletion—The full-length L1 clones of HPV11, HPV16, HPV18, and HPV35 in pGEX-2T were used as parent clones for generating the mutants. The L1 proteins were expressed as GST-L1 fusions in this *Escherichia coli* expression vector. Standard PCR with pairs of forward and reverse primers were used to amplify the clone, except for the regions to be deleted. The N-terminal 9 residues, C-terminal 31 residues, and helix 4 (residues 404–436) in HPV16 L1 are known to be required for particle assembly (15, 21). Equivalent residues on other HPV types are also deleted to prevent particle assembly. The PCR fragment with a new unique restriction site incorporated into both primers was digested with a unique enzyme for ligation. All of the deletion clones were confirmed by DNA sequencing.

Protein Purification—The protein expression and purification of all L1 deletion mutants was carried out essentially as described previously (15, 21, 22). Briefly, 0.2 mM isopropyl-β-D-thiogalactopyranoside was use to induce protein expression overnight at room temperature. After cell lysis by sonication in buffer L (50 mM Tris-HCl, pH 8.0, 0.2 M NaCl, 1 mM dithiothreitol (DTT), 1 mM EDTA, 10 mM phenylmethylsulfonyl fluoride), urea (ultrapure grade) was slowly added to the lysate to a final concentration of 3.0 M. The mixture was incubated at room temperature for 1 h with gentle shaking, and then dialyzed against three changes of buffer over 18 h. After centrifugation at 25,000 × *g* for 75 min, the supernatant was passed through a glutathione affinity column to bind GST-L1 fusion proteins. The column was washed with 10× bed volumes of buffer L to wash away contaminating proteins. L1 was then cleaved from the GST fusion using thrombin (Sigma; T6634) in an approximate ratio of 100 μg of GST-L1 to 1 NIH unit of enzyme. The digestion was carried out at 4 °C overnight. L1 pentamers were further purified by Superdex-200 (60/16 column) size exclusion chromatography.

Crystallization and Data Collection—Purified L1 pentamers of HPV11, 16, 18, and 35 were concentrated to 10–16 mg/ml in a buffer containing 20 mM Tris, pH 8.0, 50 mM NaCl, and 1 mM DTT. Crystallization trials were performed using the crystallization screens of Nextal Biotechnologies. Diffraction quality crystals were obtained by the hanging drop vapor diffusion method incubated at 18 °C for 7–10 days. HPV16 L1 was crystallized in a precipitant containing 25% polyethylene glycol 1000, 0.1 M MES, pH 6.5, and 0.1 M potassium thiocyanate. HPV18 was crystallized in the precipitant having 0.15 M sodium acetate, pH 4.6, 15% polyethylene glycol 4000, 0.16 M ammonium sulfate, 10 mM DTT, 10% glycerol, and 2.5% 1,6-hexanediol. HPV11 was crystallized in the precipitant containing 0.08 M MOPS, pH 6.5, 19% polyethylene glycol 4000, 0.4 M ammonium sulfate, 10 mM DTT, 10% glycerol, and 5% 1,6-hexanediol. HPV35 was crystallized in a precipitant containing 0.08 M sodium citrate, pH 5.6, 6% polyethylene glycol 6000, 0.45 M ammonium sulfate, 10 mM DTT, 10% glycerol. All of the crystals were flash frozen with a prior soaking in cryo-protectant containing the precipitant and 20% (v/v) glycerol.

Diffraction data for HPV11, 16, 18, and 35 L1 mutants were collected up to the resolutions of 3.2, 3.7, 3.4, and 3.5Å at syn-

Downloaded from http://www.jbc.org/ by guest on August 5, 2013

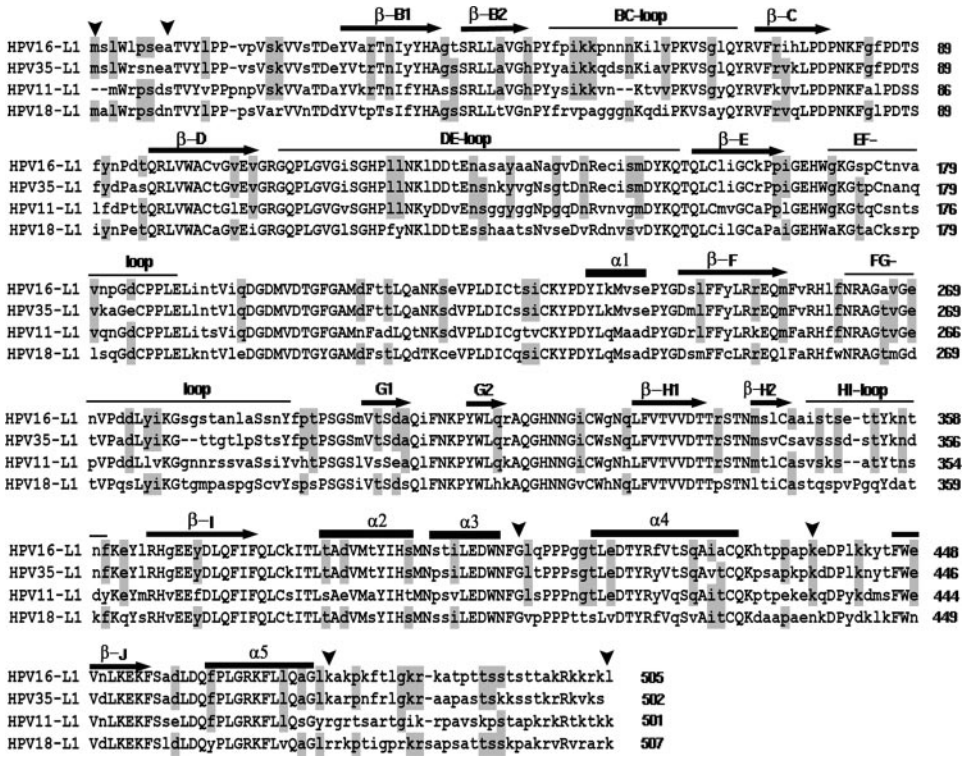

FIGURE 1. **Sequence alignment of L1 from the HPV types HPV11, HPV16, HPV18, and HPV35.** The residues conserved across four HPV types are shown in *capital letters*, whereas the nonconserved residues are given in *lowercase letters*. The residues identical among three HPV types are shown in *gray shading*. The β-sheets are shown as *arrows*. The α-helices are marked as *thick bars*. The five loops displayed on the surface of the virus particle are marked and labeled. The regions in between the marks (▼) at the N terminus, C terminus, and helix 4 are deleted in our constructs.

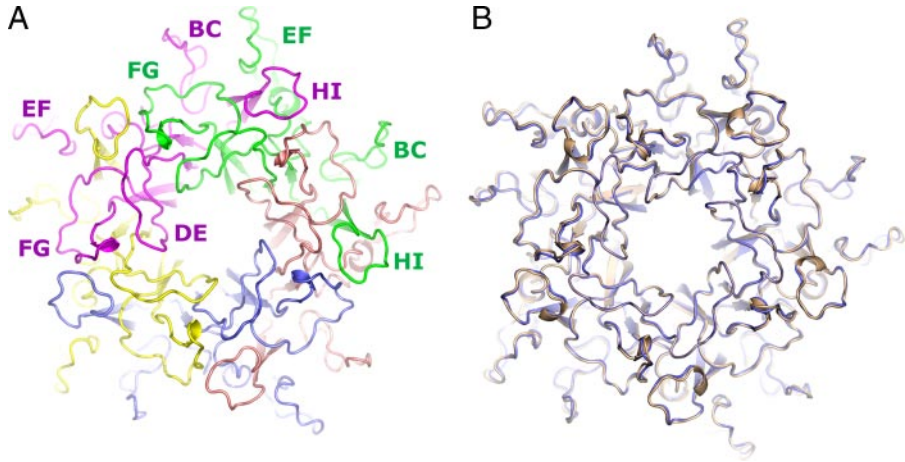

FIGURE 2. *A*, the crystal structure of HPV16 L1 pentamer, where each monomer is shown in different color to show the intertwining of the surface loops. *B*, superposition of HPV16 L1 pentamer (*violet*) on the pentamer taken from T = 1 particle assembly of HPV16 (*brown*).

chrotron beamlines of the Advanced Light Source (Berkeley). The data were processed using HKL2000. The data statistics are given in Table 1.

Structure Determination and Refinement—L1 pentamer structures of all four types were solved by Molecular Replacement using MOLREP of CCP4 suite. The pentameric model obtained from HPV16 L1 T = 1 structure (Protein Data Bank code 1DZL) was used as a search model, yielding three pentamers in the asymmetric unit for HPV16, HPV18, and HPV35 with space group $P2_12_12_1$, P1, and $P2_1$, respectively. HPV11 L1 crystallized in the space group C2 with one pentamer in the asymmetric unit. The structures were refined by alternating cycles of model rebuilding and refinement using O, CNS, and REFMAC. With three pentamers in one asymmetric unit for HPV16, HPV18, and HPV35, we used 15-fold noncrystallographic symmetry at early stage of refinement, whereas 5-fold noncrystallographic symmetry was used for HPV11. Cycles of positional refinement combined with simulated annealing refinement produced good R_{free} value for all the four structures (Table 1). The final structures of each types have been validated by using omit map in CNS, which produced excellent electron density maps for the L1 pentamers of each type.

Selected mAb Binding to L1 Pentamers—Various mAbs detecting type-specific conformational and cross-reactive linear epitopes of HPV11, 16, and 18 were tested by enzyme-linked immunosorbent assay for reactivity to pentamers. The mAbs used in this study were derived from mice immunized with HPV16 and HPV18 L1 VLP antigens (18, 23) or HPV11 virions (10). All of the mAbs recognize L1 epitopes that are either conformational or linear, and the binding and neutralization properties of these mAbs have been described previously (23).

Both intact pentamers (attached to enzyme-linked immunosorbent assay plate wells at 1 μg/well in phosphate-buffered saline, pH 7.0) and denatured pentamers (attached at 1 μg/well in alkaline buffer, pH 9.5, containing dithiothreitol) were tested in duplicate. Each mAb supernatant was tested at dilutions of 1:50, and means (±S.D.) of optical densities calculated as previously described (23). Additional experiments were set up to compare binding of mAbs to pentamers *versus* baculovirus-derived L1 VLPs.

RESULTS

Protein Expression, Purification, Crystallization, and Structure Determination—The constructs of the major capsid protein L1 of HPV11, 16, 18, and 35, all of which have deletions of 9 residues at the N terminus, 31 residues at the C

Downloaded from http://www.jbc.org/ by guest on August 5, 2013

TABLE 2

Binding results of NmAbs with the assembly-deficient L1 pentamers

The optical density reading reflecting significant binding between the mAbs and the free pentamers are underlined.

Neutralizing mAbs (epitope type)	Optical densities			
	35 Pentamer	11 Pentamer	16 Pentamer	18 Pentamer
		Mean ± S.D.		
H11.B2 (Conf.)[a]	0.002 (0.001)	1.112 (0.050)	0.000 (0.000)	0.001 (0.001)
H11.F1 (Conf.)		0.691 (0.080)		
H6.C6 (Linear)[b]		0.002 (0.001)		
H16.V5 (Conf.)	0.000 (0.001)	0.002 (0.001)	0.554 (0.057)	0.002 (0.001)
H16.6F (Conf.)			0.282 (0.004)	
H16.D9 (Linear)		0.147 (0.005)	0.075 (0.002)	
H16.J4 (Linear)	0.113 (0.010)	0.001 (0.000)	0.262 (0.006)	0.004 (0.001)
H18.J4 (Conf.)	0.002 (0.000)	0.001 (0.000)	0.001 (0.000)	0.558 (0.057)
H18.K2 (Conf.)				0.127 (0.026)
H18.F8 (Conf.)				1.423 (0.047)
H18.L9 (Linear)				0.332 (0.007)

[a] Conformational epitope.
[b] Linear epitope.

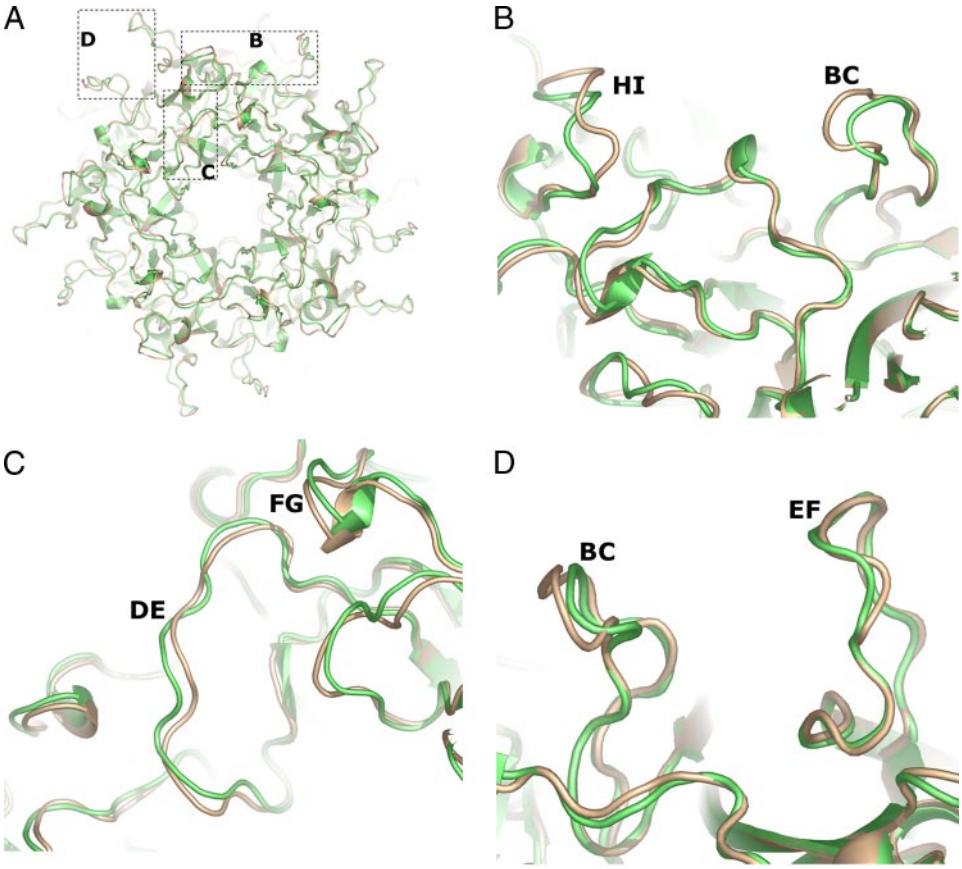

FIGURE 3. **Comparison of HPV11 L1 pentamer (*green*) with HPV16 L1 pentamer (*brown*).** *A*, overall superposition of HPV11 L1 pentamer on that of HPV16. The *boxed areas* indicate locations of *B–D*. *B*, HI and BC loops are shorter in HPV11 compared with HPV16. *C*, the structural difference of DE loop between HPV11 and HPV16. *D*, the EF loop of HPV11 is similar in conformation to that of HPV16.

terminus, and the helix 4 (α4; residues 404–436, HPV16 L1 numbering) (Fig. 1), were expressed as GST fusion proteins in *E. coli*. The α4 and the N terminus of L1 have been implicated in VLP formation (15), and the truncation of these motifs produced only pentamers of L1 that could not assemble in VLP (21). The assembly-deficient pentamers of these four types were crystallized into four different space groups (Table 1).

All four L1 pentamer structures were solved by Molecular Replacement using the coordinates of an L1 pentamer taken from the T = 1 particle structure of HPV16 L1 as a search model (Protein Data Bank code 1DZL (15)). The L1 pentamers of each HPV type had a different crystal packing, forming head-head, tail-tail, or side-side interactions between pentamers (supplemental Fig. S1). The L1 pentamer structures of HPV11, HPV16, HPV18, and HPV35 were refined to 3.2, 3.7, 3.4, and 3.3 Å, respectively (Table 1). The electron density maps are all very well featured, because of the powerful phase improvement method of 5–15-fold noncrystallographic symmetry averaging used here, which allow us to confidently locate the residues not only at the core regions but also at the surface loops, even at these resolutions. Excellent side chain electron density maps have been produced previously by multi-fold noncrystallographic symmetry averaging at 4.7 Å for P97 protein (24) and at 3.5 Å for our previous L1 structure in T1 papillomavirus particle in which the density map at 4.5 Å had the quality comparable with those near 3.0 Å (15).

Overall Pentamer Structure—L1 pentamer structures of all four HPV types grossly resemble the pentamer structure of T = 1 HPV16 L1. The HPV16 L1 free pentamer structure is shown in Fig. 2*A* as a representative of the four pentamer structures. In brief, five monomers are assembled in symmetrical manner to form the pentamer with a hollow channel at the center through a 5-fold central axis. The backbones of the polypeptide chain of the adjacent subunit interact

Downloaded from http://www.jbc.org/ by guest on August 5, 2013

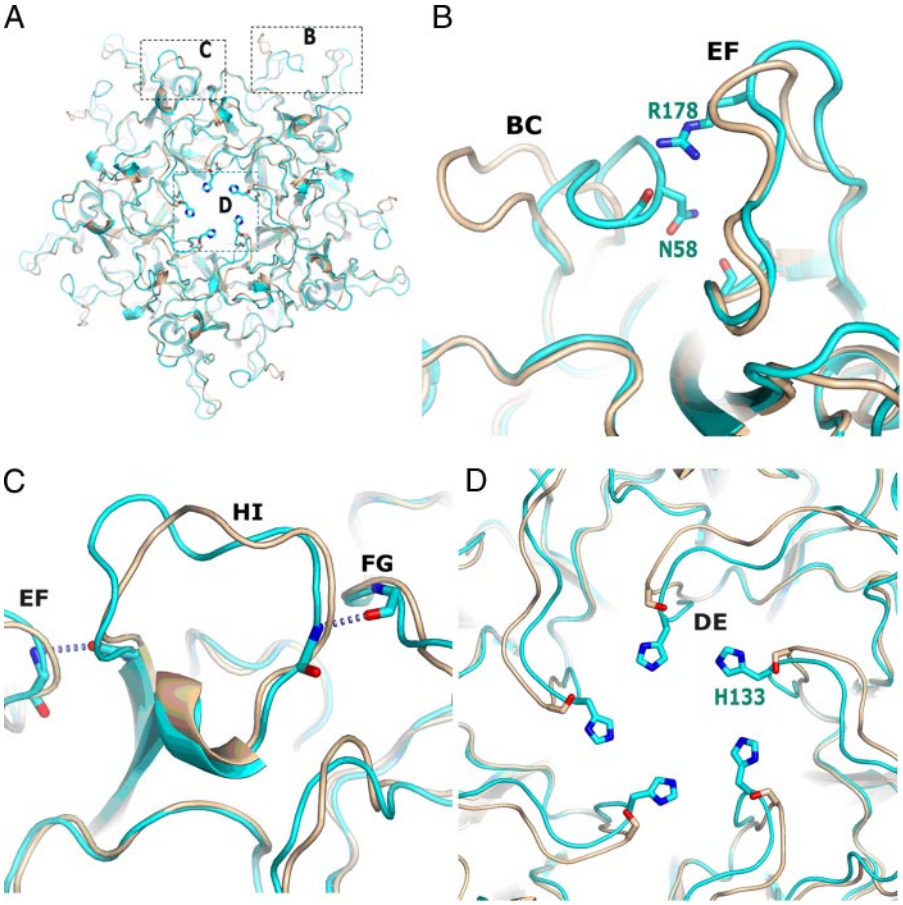

FIGURE 4. **Comparison of HPV18 L1 pentamer (*cyan*) with HPV16 L1 pentamer (*brown*).** *A*, overall superposition of HPV18 L1 pentamer on that of HPV16. The *boxed areas* indicate locations of *B–D*. *B*, structural differences of BC and EF loops between HPV18 and HPV16 L1. In HPV18, Asn^{58} and Gly^{57} of the BC loop form hydrogen bonds with Arg^{178} and Cys^{185} of the EF loop, *C*, HI loop forms hydrogen bonds with EF and FG loops at backbone level in both HPV18 and HPV16 pentamers (shown for HPV18). *D*, the structural difference of the DE loop, resulting in a narrower central channel for HPV18 L1 pentamer having a diameter of 10 Å, whereas this diameter is 18 Å for HPV16.

directly, and the surface loops show elaborate intertwining between the individual monomers.

BC, DE, EF, FG, and HI are the five loops displayed on the surface of the pentamer (Fig. 2*A*). Thus, these five loops constitute the part of the viral surface that can be recognized as conformational epitopes of HPV. The overall arrangements of these surface loops are grossly similar for all four HPV types. Briefly, the HI loop of one monomer inserts between the FG and EF loops of its clockwise (surface view) neighbor and reaches far enough to contact the FG loop of the next neighbor (Fig. 2*A*). The BC and EF loops from two neighboring monomers are juxtaposed on the outer rim of the pentamer (Fig. 2*A*). The DE loop encircles the exposed surface around the rim of the central hollow channel. The FG loop can be divided into early and late regions; the early region (residues 264–278, HPV16 numbering) decorates the base of the juxtaposed BC and EF loops, whereas the late region (residues 279–288, HPV16 numbering) inserts between the DE and HI loops (Fig. 2*A*).

Free Pentamer Structure versus the T = 1 Particle Pentamer for HPV16—To examine whether the assembly-deficient L1 pentamer has the same structure as the pentamer capable of assembly into T = 1 particles, we determined the structure of HPV16 L1 as free pentamers and compared it with the pentamer structure in the T = 1 particle (Fig. 2*B*). Superimposition of the core β-sheets of the free pentamer structure on the pentamer of T = 1 particle revealed essentially identical conformation (root mean square deviation, 0.32 Å) not only for the core structure but also for the five surface loops (Fig. 2*B*), which were not used for the superposition, demonstrating that neither the internal deletion of helix 4 (α4) of L1 nor the different crystal packing changed the β-sheet core and more importantly the surface loop structure of HPV16 L1 pentamer. This result suggests that the loop structures are tightly anchored on to the surface of L1 pentamer, and their conformations are stably maintained as free pentamers in solution as well as in different crystal packing. The conformational integrity and stability of the assembly-deficient pentamers were also confirmed by their ability to bind a battery of NmAbs, raised against VLPs.

Binding of Free Pentamers with NmAbs Raised against VLPs of Different HPV Types—The discovery of no significant differences between the crystal structures of HPV16 L1 from the free pentamer and the pentamer in the T = 1 particle demonstrates that the helix 4 deletion, which results in free pentamers, does not lead to significant conformational changes. Therefore, it is reasonable to conclude that the surface loop conformational changes between different HPV L1 pentamers reflect the true structural differences on the viral surface of these HPV types.

To provide further experimental support for this conclusion, a panel of available NmAbs raised against VLPs was tested for binding the free pentamers (Table 2). The results showed that most of the NmAbs with conformational epitopes had strong type-specific binding with the free pentamer (Table 2), suggesting that the conformations of the viral surface loops on pentamers are maintained as in the VLPs. The linear epitope mAbs H6.C6 did not bind the pentamers, H6.C6 is known to be specific to the first 10 amino acids at the N terminus. Thus, it is expected that this mAb should not bind the free pentamer of HPV11 that lacks the first 10 N-terminal residues. H16.J4, a linear epitope mAb of HPV16, showed some weak cross-type reactivity with HPV35 L1 (Table 2). However, all the conformational epitope mAbs reacted only to the corresponding HPV types. The locations for the conformational epitopes for the

Downloaded from http://www.jbc.org/ by guest on August 5, 2013

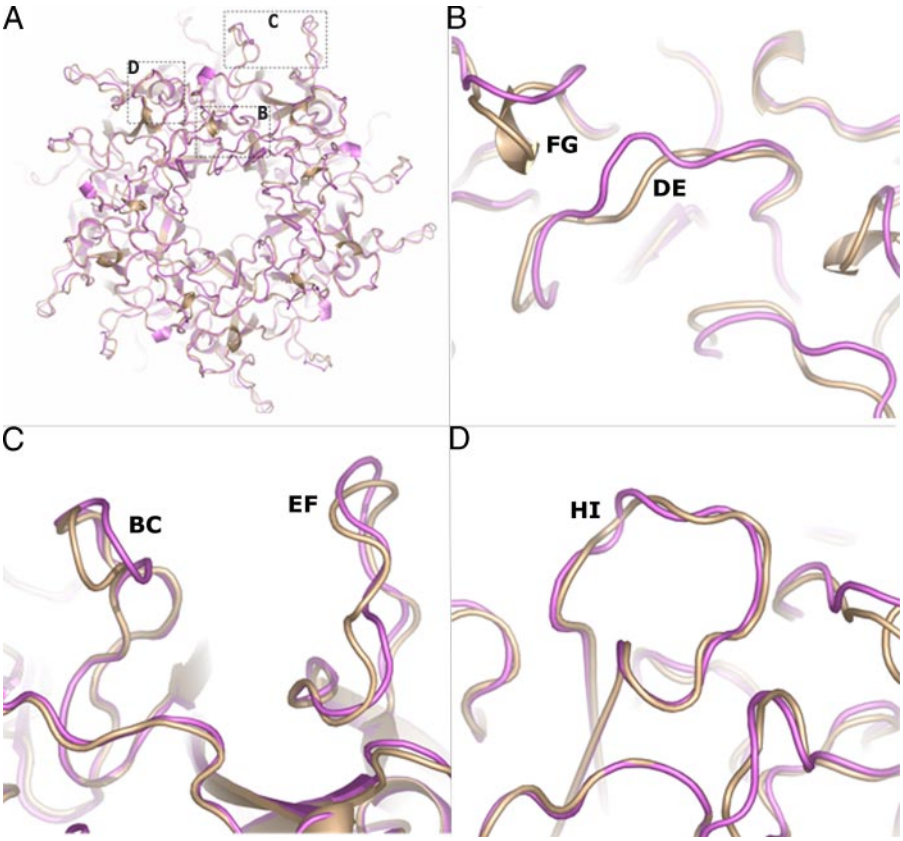

FIGURE 5. **Comparison of HPV35 L1 pentamer (*violet*) with HPV16 L1 pentamer (*brown*).** *A*, overall superposition of HPV35 L1 pentamer on that of HPV16. The *boxed areas* indicate locations of *B–D*. *B*, structural differences in DE and FG loops between HPV35 and HPV16. *C*, structural differences in BC and EF loops between HPV35 and HPV16. *D*, subtle difference in conformation between the HI loops of HPV16 and HPV35 L1.

NmAbs are all accessible from the top surface of L1 pentamers for the different HPV types.

Structural Comparison between the L1 Pentamers from Different HPVs—The surface loops of HPV16, either in free pentamers or in the HPV16 T = 1 particle, show identical conformations, which convinced us that the observed loop conformations in the pentamers are not influenced either by the crystal packing or the deletion of the residues at the N and C termini and helix 4. Binding results of the pentamers with NmAbs (Table 2) further supported the fact that the surface loops of the free pentamers are functionally as potent as their corresponding VLPs, and the surface of the free pentamer correctly represents the surface of VLPs or the capsids.

We have performed a pairwise structural comparison of HPV11, HPV18, and HPV35 pentamers with the pentamer taken from HPV16 T = 1 particle by superposition based on the two core β-sheets from each monomer.

HPV11 versus HPV16 L1 Pentamers—The pentameric structure of HPV11 L1 was compared with that of HPV16, and the root mean square deviation of the superposition was 0.38 Å, indicating that the β-sheet core structures are almost identical for HPV11 and HPV16 (Fig. 3*A*). However, structural differences for the loops, located on the pentamer surface, are obvious in the superposition (Fig. 3, *B* and *C*). The BC and HI loops of HPV11 are 3.5 and 2.0 Å shorter than the corresponding loops of HPV16 L1 (Fig. 3*B*), which correlates with the amino acid deletion in these two loops of HPV11 L1 (Fig. 1). Such structural differences of the two loops are expected to exhibit distinct protein-protein interaction specificity in their antibody binding.

Structural differences are also observed in the DE loop (Fig. 3*C*), and distinct amino acid sequence differences between the two types were observed. For example, the residues corresponding to Gly^{133}, Gly^{134}, and Pro^{136} on the DE loop of HPV11 L1 are all Ala in HPV16 (Fig. 1). Because Gly and Pro are known to exert local structural perturbation, because of either the known flexibility or lack of an amide hydrogen, the observed conformational difference of the DE loop of HPV11 L1 from that of HPV16 L1 is expected in this case. However, the EF loop conformation of HPV11 L1 is similar to that of HPV16 L1 (Fig. 3*D*).

HPV18 Versus HPV16 L1 Pentamers—The β-sheet core of the HPV18 L1 pentamer superimposes well with HPV16 L1, with a root mean square deviation of 0.47 Å. However, substantial structural differences were observed for all five surface loops (Fig. 4). The BC loop of HPV18 L1 shows a drastically different conformation, with its tip oriented ~13 Å away from the corresponding loop of HPV16 L1 (Fig. 4*B*). The deviation of BC loop of HPV18 starts from Pro^{53}, unique to HPV18, whereas the deviation ends at Pro^{63} conserved in all four types. This conformational shift of the BC loop has been accommodated through a lateral displacement of the adjacent EF loop, moving in a concerted manner in the same direction, where the residues of the EF loop have been shifted by ~4 Å from that of HPV16 (Fig. 4*B*). This shift of BC and EF loops in HPV18 L1 places the two loops in close contact, allowing the formation of a number of hydrogen bonding interactions between the residues from the BC and EF loops (Fig. 4*B*).

The conformation of the HI loop of HPV18 L1 is significantly different from the HI loop of HPV16 L1 (Fig. 4*C*), which may be the result of the combined effect of an amino acid insertion and the presence of two Pro residues at successive positions (351 and 353) in HPV18 L1 compared with HPV16. Interestingly, the HI loop in HPV11, 16, and 18 forms hydrogen bonds with the EF on one side and with FG loops on the other side (Fig. 4*C*), which may help stabilize the HI loop conformation on the surface.

Downloaded from http://www.jbc.org/ by guest on August 5, 2013

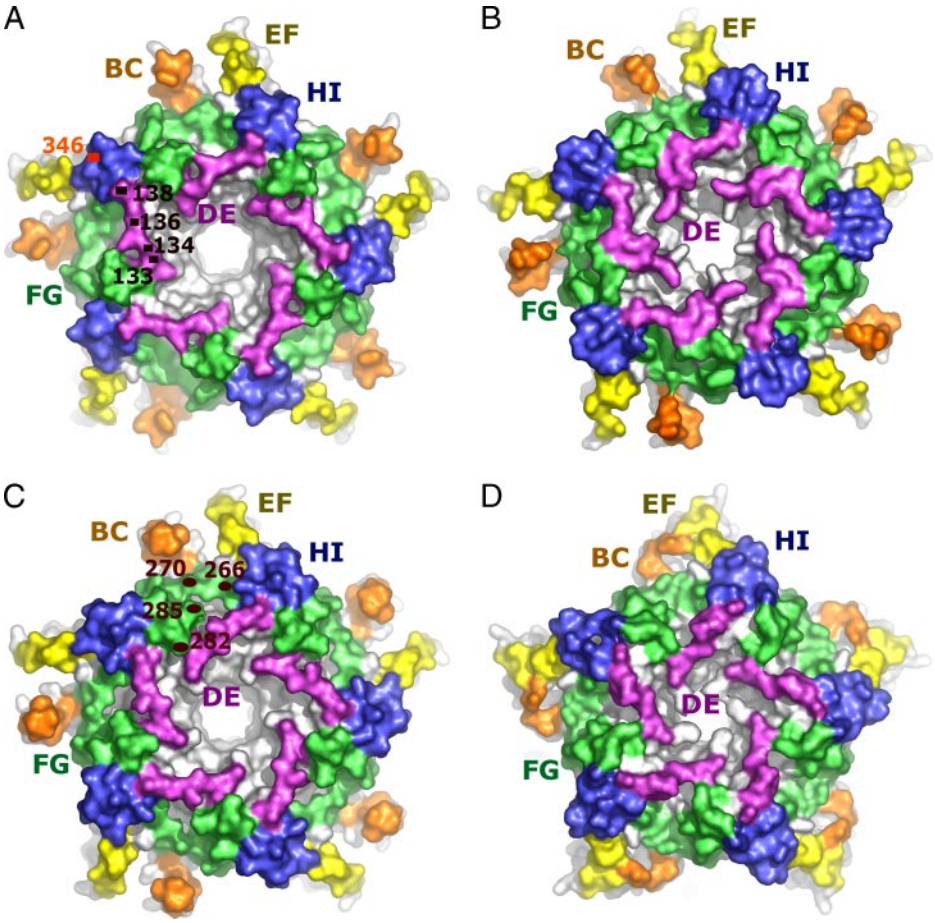

FIGURE 6. **Surface representation of L1 pentamers from four HPV types.** The surface loops are colored differently on the surface: BC (*orange*), DE (*violet*), EF (*yellow*), FG (*green*), and HI (*slate*). *A*, HPV11; *B*, HPV35; *C*, HPV16; *D*, HPV18 L1. The distinct structural features can be observed for the surface loops among the four HPV types. Neutralizing epitopes are shown schematically on HPV11 and HPV16 pentamers. *Black square*, H11.F1 and H11.G5; *orange square*, H11.H3; *red ellipse*, H16.V5 and H16.E70.

The DE loop is located on the inner channel ridge of the L1 pentamer. The diameter of the pentamer channel is ~18 Å for HPV16 L1, but it narrows down to 10 Å in HPV18 L1 (Fig. 4*D*). This narrowing of the pentameric channel in HPV18 L1 is caused by the shifting of DE loop toward the channel center. The residue His^{133} located at the narrowest point of the channel is protruding into the channel space (Fig. 4*D*).

HPV35 Versus HPV16 L1 Pentamers—The superposition of HPV35 L1 over the β sheet core of HPV16 L1 produced a root mean square deviation of 0.38 Å, indicating a very similar core structure (Fig. 5*A*). However, the superposition reveals different structural features for the surface loops. The FG loop of HPV35 has a two-residue deletion compared with HPV16 (as well as HPV11 and HPV18) (Fig. 1), which results in the structural difference of this loop (Fig. 5*B*). The region of the DE loop in proximity of the FG loop also shows a structural change compared with HPV16. It appears that the 133–141 region of the DE loop of HPV35 L1 moves toward the FG loop (Fig. 5*B*). Structural differences are observed for both the BC and EF loops between HPV 35 and HPV16 (Fig. 5*C*). Subtle but significant conformational changes are observed for the HI loop. In addition to the conformational difference, the orientation of different amino acid side chains on the tip of HI loop accounts for the major differences between these two HPV types (Fig. 5*D*).

DISCUSSION

In this study, we have determined the crystal structures of L1 pentamers of four different HPV types (among which HPV11, HPV18, and HPV35 L1 structures were determined for the first time), to elucidate their detailed structural features at the capsid surface that control their specific pathogenicity and antigenic property. We have observed that although the β-sheet core structures of the L1 pentamers of the four HPV types are nearly identical, the loop structures on the pentamer surfaces display significant conformational differences (Figs. 3–5). The high type specificity of the conformational epitope NmAbs we tested here supportively suggests that a few angstrom shift of the surface loop or a few substitutions of the surface loop residues can lead to changes of the viral surface antigen determinants in eliciting different antibodies, as well as to the disruption of binding with a mAb that recognizes the same location on the pentamer surface of another HPV type.

Pairwise comparisons reveal that the extent of conformational changes for a particular loop is different for different pairs. The loops with a few insertions or deletions of amino acids expectedly showed moderate spatial shifts (of ~4 Å), but the extent and the direction of large structural differences (that range up to 7–15 Å), as observed in HPV18 and HPV35, were not predictable from their primary sequences. The conformational differences of the surface loops can also be visualized in the surface representation of the pentamer structures in Fig. 6. Because most of the known epitopes for the available NmAbs are located on the surface loops, the distinct structural features of these surface loops might be expected to form distinct surface conformational epitopes.

A minor structural difference of the epitope loop, with a spatial shift of ~2 Å, is found to be sufficient to disrupt the antibody-epitope binding. Such a disruption of antibody binding is further amplified by the substitution of one or more residues on the loops from different HPV types. This change is evident in the structural differences in the DE loop between HPV11 and HPV16, where a combination of the structural shift of the DE loop (Fig. 3) with a three-residue substitution from Gly-Gly-Pro in HPV11 to Ala-Ala-Ala in HPV16 produced a rather distinct structural feature for the DE loop (Figs. 3 and 6), abrogating the

Downloaded from http://www.jbc.org/ by guest on August 5, 2013

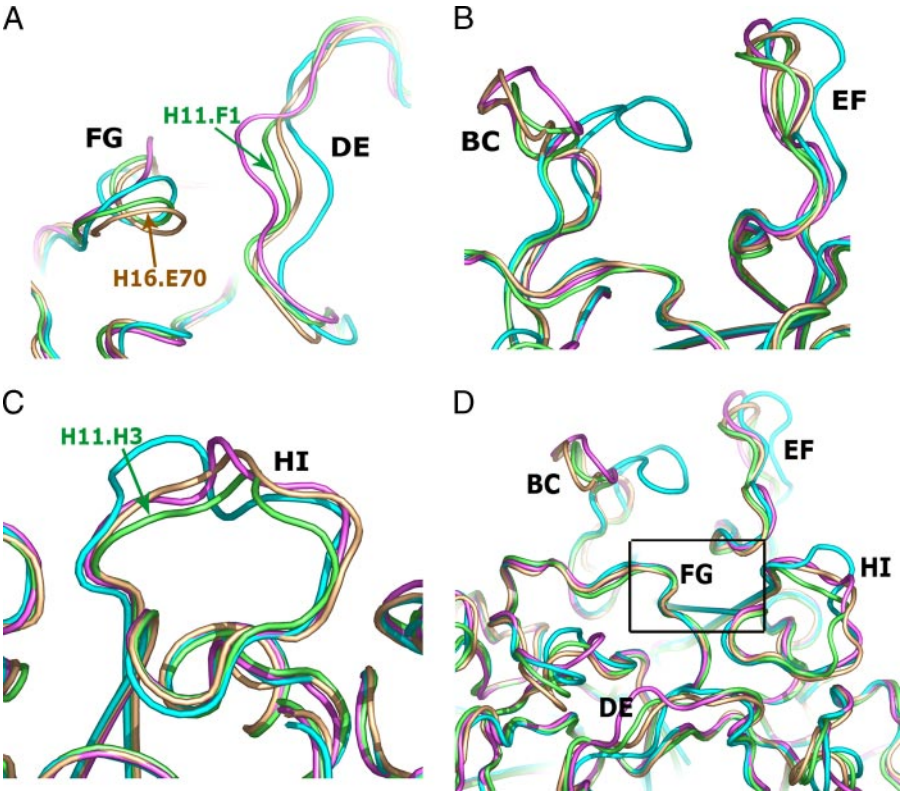

FIGURE 7. **Comparison of L1 pentamer surfaces of HPV11 (*green*), HPV16 (*brown*), HPV18 (*cyan*), and HPV35 (violet).** *A*, the structural differences in the DE loop and the late region of the FG loop are shown here. The known epitopes of the mAbs H11.F1 and H16.E70 are marked. *B*, conformational differences of BC and EF loops of four HPV types are shown. *C*, conformational difference in HI loop is shown. The epitope of H11.H3 is marked. *D*, superposition of four pentamers to show the region structurally similar in all (marked in a *box*).

binding of HPV11 DE loop specific NmAbs, H11.F1, and H11.G5 to HPV16.

This finding implies that antibody binding is very precise in HPVs, and perturbation of a small part of the binding interface by replacing amino acid side chains or by shifting the loop position by only 1–2 Å at the binding interface appears to be significant in determining the binding by the NmAbs. Comparison of the pentameric surfaces of all four types (Fig. 7) reveals even more interesting features compared with the pairwise comparisons. For example, Fig. 7*A* shows that the DE loop of HPV11 that contains the epitope for H11.F1 is conformationally far apart from HPV18 and HPV35, which correlates with our mAb binding study (Table 2) and convincingly rules out the possibility of any cross-reactivity at this site.

Similarly, FG loop of HPV35 posses a distinguished conformation compared with the FG loop of HPV16, which contains a known epitope for HPV16.E70 (Fig. 7*A*). Rather, the orientation of the late region of FG loop coupled with the orientation of adjacent DE loop form a distinct structural feature. The distance between these loops widely vary in the four HPV types being the maximum (~15 Å) in HPV18 and the minimum (~7 Å) in HPV35. A notable conformational difference is also observed at the tip of the HI loop of the four types (Fig. 7*C*) that contains a known epitope for NmAb H11.H3. These phenomena may collectively explain why no cross-reactivity between HPV types is observed for the NmAbs with conformational epitopes on the viral surface.

However, there are parts on the pentamer surface area, such as the base of the HI loop and the early region of the FG loop (Fig. 7*D*), which have essentially identical structures among the different types. If epitopes in these areas can elicit antibody production as strong antigen determinants, these epitopes are expected to be cross-reactive between types and offer cross-protection as vaccine. Nonetheless, no cross-reactive NmAbs with conformational epitopes have been identified yet, which may suggest that these "common" epitopes may not have strong antigenicity or may be sterically inaccessible. In conclusion, despite the high sequence homology of L1 proteins between different types and the overall structural conservation of L1 pentamers, the detailed loop structures on the pentamer (and thus viral) surface are largely different because of their different amino acid composition and insertions/deletions, which not only change the surface epitope composition and conformation but also affect the viral surface antigenicity, providing a molecular rationalization for the type specificity of NmAbs.

Acknowledgments—We thank the staff at synchrotron beamlines 4.2.2, 5.0.2, 8.2.1, and 8.2.2 in the Advanced Light Source at Berkeley for assistance in data collection.

REFERENCES

1. Munoz, N., Bosch, F. X., de Sanjose, S., Herrero, R., Castellsague, X., Shah, K. V., Snijders, P. J., and Meijer, C. J. (2003) *N. Engl. J. Med.* **348,** 518–527
2. Ho, G. Y., Bierman, R., Beardsley, L., Chang, C. J., and Burk, R. D. (1998) *N. Engl. J. Med.* **338,** 423–428
3. Lowy, D. R., and Howley, P. M. (2001) *Papillomaviruses and Their Replication*, Lippincot Williams & Wilkins, Philadelphia, PA
4. Kirnbauer, R., Booy, F., Cheng, N., Lowy, D. R., and Schiller, J. T. (1992) *Proc. Natl. Acad. Sci. U. S. A.* **89,** 12180–12184
5. Hagensee, M. E., Yaegashi, N., and Galloway, D. A. (1993) *J. Virol.* **67,** 315–322
6. Kirnbauer, R., Taub, J., Greenstone, H., Roden, R., Durst, M., Gissmann, L., Lowy, D. R., and Schiller, J. T. (1993) *J. Virol.* **67,** 6929–6936
7. Rose, R. C., Reichman, R. C., and Bonnez, W. (1994) *J. Gen. Virol.* **75,** 2075–2079
8. Zhou, J., Stenzel, D. J., Sun, X. Y., and Frazer, I. H. (1993) *J. Gen. Virol.* **74,** 763–768
9. Harro, C. D., Pang, Y. Y., Roden, R. B., Hildesheim, A., Wang, Z., Reynolds, M. J., Mast, T. C., Robinson, R., Murphy, B. R., Karron, R. A., Dillner, J., Schiller, J. T., and Lowy, D. R. (2001) *J. Natl. Cancer Inst.* **93,** 284–292
10. Christensen, N. D., and Kreider, J. W. (1990) *J. Virol.* **64,** 3151–3156
11. Christensen, N. D., Kreider, J. W., Cladel, N. M., and Galloway, D. A. (1990) *Virology* **175,** 1–9
12. Christensen, N. D., Kirnbauer, R., Schiller, J. T., Ghim, S. J., Schlegel, R.,

Downloaded from http://www.jbc.org/ by guest on August 5, 2013

Jenson, A. B., and Kreider, J. W. (1994) *Virology* **205,** 329–335
13. White, W. I., Wilson, S. D., Bonnez, W., Rose, R. C., Koenig, S., and Suzich, J. A. (1998) *J. Virol.* **72,** 959–964
14. White, W. I., Wilson, S. D., Palmer-Hill, F. J., Woods, R. M., Ghim, S. J., Hewitt, L. A., Goldman, D. M., Burke, S. J., Jenson, A. B., Koenig, S., and Suzich, J. A. (1999) *J. Virol.* **73,** 4882–4889
15. Chen, X., Garcea, R., Golderg, I., Casini, G., and Harrison, S. C. (2000) *Mol. Cell* **5,** 557–567
16. Sadeyen, J. R., Tourne, S., Shkreli, M., Sizaret, P. Y., and Coursaget, P. (2003) *Virology* **309,** 32–40
17. Slupetzky, K., Shafti-Keramat, S., Lenz, P., Brandt, S., Grassauer, A., Sara, M., and Kirnbauer, R. (2001) *J. Gen. Virol.* **82,** 2799–2804
18. Christensen, N. D., Cladel, N. M., Reed, C. A., Budgeon, L. R., Embers, M. E., Skulsky, D. M., McClements, W. L., Ludmerer, S. W., and Jansen, K. U. (2001) *Virology* **291,** 324–334
19. Ludmerer, S. W., Benincasa, D., and Mark, G. E., III (1996) *J. Virol.* **70,** 4791–4794
20. Ludmerer, S. W., Benincasa, D., Mark, G. E., III, and Christensen, N. D. (1997) *J. Virol.* **71,** 3834–3839
21. Bishop, B., Dasgupta, J., and Chen, X. S. (2007) *Virol. J.* **4,** 3
22. Chen, X., Casini, G., Harrison, S. C., and Garcea, R. (2001) *J. Mol. Biol.* **307,** 173–182
23. Christensen, N. D., Dillner, J., Eklund, C., Carter, J. J., Wipf, G. C., Reed, C. A., Cladel, N. M., and Galloway, D. A. (1996) *Virology* **223,** 174–184
24. DeLaBarre, B., and Brunger, A. T. (2003) *Nat. Struct. Biol.* **10,** 856–863

Downloaded from http://www.jbc.org/ by guest on August 5, 2013